

Observation of resonant contribution to the $e^+e^- \rightarrow \Omega^-\bar{\Omega}^+$ around 4.2 GeV and evidence of $\psi(3770) \rightarrow \Omega^-\bar{\Omega}^+$

M. Ablikim¹, M. N. Achasov^{4,b}, P. Adlarson⁷⁵, O. Afedulidis³, X. C. Ai⁸⁰, R. Aliberti³⁵, A. Amoroso^{74A,74C}, Q. An^{71,58}, Y. Bai⁵⁷, O. Bakina³⁶, I. Balossino^{29A}, Y. Ban^{46,g}, H.-R. Bao⁶³, V. Batozskaya^{1,44}, K. Begzsuren³², N. Berger³⁵, M. Berlowski⁴⁴, M. Bertani^{28A}, D. Bettone^{29A}, F. Bianchi^{74A,74C}, E. Bianco^{74A,74C}, A. Bortone^{74A,74C}, I. Boyko³⁶, R. A. Briere⁵, A. Brueggemann⁶⁸, H. Cai⁷⁶, X. Cai^{1,58}, A. Calcaterra^{28A}, G. F. Cao^{1,63}, N. Cao^{1,63}, S. A. Cetin^{62A}, J. F. Chang^{1,58}, W. L. Chang^{1,63}, G. R. Che⁴³, G. Chelkov^{36,a}, C. Chen⁴³, C. H. Chen⁹, Chao Chen⁵⁵, G. Chen¹, H. S. Chen^{1,63}, M. L. Chen^{1,58,63}, S. J. Chen⁴², S. L. Chen⁴⁵, S. M. Chen⁶¹, T. Chen^{1,63}, X. R. Chen^{31,63}, X. T. Chen^{1,63}, Y. B. Chen^{1,58}, Y. Q. Chen³⁴, Z. J. Chen^{25,b}, Z. Y. Chen^{1,63}, S. K. Choi^{10A}, X. Chu⁴³, G. Cibinetto^{29A}, F. Cossio^{74C}, J. J. Cui⁵⁰, H. L. Dai^{1,58}, J. P. Dai⁷⁸, A. Dbeysi¹⁸, R. E. de Boer³, D. Dedovich³⁶, C. Q. Deng⁷², Z. Y. Deng¹, A. Denig³⁵, I. Denysenko³⁶, M. Destefanis^{74A,74C}, F. De Mori^{74A,74C}, B. Ding^{66,1}, X. X. Ding^{46,g}, Y. Ding³⁴, Y. Ding⁴⁰, J. Dong^{1,58}, L. Y. Dong^{1,63}, M. Y. Dong^{1,58,63}, X. Dong⁷⁶, M. C. Du¹, S. X. Du⁸⁰, Z. H. Duan⁴², P. Egorov^{36,a}, Y. H. Fan⁴⁵, J. Fang^{1,58}, J. Fang⁵⁹, S. S. Fang^{1,63}, W. X. Fang¹, Y. Q. Fang^{1,58}, R. Farinelli^{29A}, L. Fava^{74B,74C}, F. Feldbauer³, G. Felici^{28A}, C. Q. Feng^{71,58}, J. H. Feng⁵⁹, Y. T. Feng^{71,58}, K. Fischer⁶⁹, M. Fritsch³, C. D. Fu¹, J. L. Fu⁶³, Y. W. Fu¹, H. Gao⁶³, Y. N. Gao^{46,g}, Yang Gao^{71,58}, S. Garbolino^{74C}, I. Garzia^{29A,29B}, L. Ge⁸⁰, P. T. Ge⁷⁶, Z. W. Ge⁴², C. Geng⁵⁹, E. M. Gersabeck⁶⁷, A. Gilman⁶⁹, K. Goetzen¹³, L. Gong⁴⁰, W. X. Gong^{1,58}, W. Gradl³⁵, S. Gramigna^{29A,29B}, M. Greco^{74A,74C}, M. H. Gu^{1,58}, Y. T. Gu¹⁵, C. Y. Guan^{1,63}, Z. L. Guan²², A. Q. Guo^{31,63}, L. B. Guo⁴¹, M. J. Guo⁵⁰, R. P. Guo⁴⁹, Y. P. Guo^{12,f}, A. Guskov^{36,a}, J. Gutierrez²⁷, K. L. Han⁶³, T. T. Han¹, X. Q. Hao¹⁹, F. A. Harris⁶⁵, K. K. He⁵⁵, K. L. He^{1,63}, F. H. Heinsius³, C. H. Heinz³⁵, Y. K. Heng^{1,58,63}, C. Herold⁶⁰, T. Holtmann³, P. C. Hong^{12,f}, G. Y. Hou^{1,63}, X. T. Hou^{1,63}, Y. R. Hou⁶³, Z. L. Hou¹, B. Y. Hu⁵⁹, H. M. Hu^{1,63}, J. F. Hu^{56,i}, T. Hu^{1,58,63}, Y. Hu¹, G. S. Huang^{71,58}, K. X. Huang⁵⁹, L. Q. Huang^{31,63}, X. T. Huang⁵⁰, Y. P. Huang¹, T. Hussain⁷³, F. Hölkzen³, N. Hüsken^{27,35}, N. in der Wiesche⁶⁸, M. Irshad^{71,58}, J. Jackson²⁷, S. Janchiv³², J. H. Jeong^{10A}, Q. Ji¹, Q. P. Ji¹⁹, W. Ji^{1,63}, X. B. Ji^{1,63}, X. L. Ji^{1,58}, Y. Y. Ji⁵⁰, X. Q. Jia⁵⁰, Z. K. Jia^{71,58}, D. Jiang^{1,63}, H. B. Jiang⁷⁶, P. C. Jiang^{46,g}, S. S. Jiang³⁹, T. J. Jiang¹⁶, X. S. Jiang^{1,58,63}, Y. Jiang⁶³, J. B. Jiao⁵⁰, J. K. Jiao³⁴, Z. Jiao²³, S. Jin⁴², Y. Jin⁶⁶, M. Q. Jing^{1,63}, X. M. Jing⁶³, T. Johansson⁷⁵, S. Kabana³³, N. Kalantar-Nayestanaki⁶⁴, X. L. Kang⁹, X. S. Kang⁴⁰, M. Kavatsyuk⁶⁴, B. C. Ke⁸⁰, V. Khachatryan²⁷, A. Khoukaz⁶⁸, R. Kiuchi¹, O. B. Kolcu^{62A}, B. Kopf³, M. Kuessner³, X. Kui^{1,63}, N. Kumar²⁶, A. Kupsc^{44,75}, W. Kühn³⁷, J. J. Lane⁶⁷, P. Larin¹⁸, L. Lavezzi^{74A,74C}, T. T. Lei^{71,58}, Z. H. Lei^{71,58}, H. Leithoff³⁵, M. Lellmann³⁵, T. Lenz³⁵, C. Li⁴⁷, C. Li⁴³, C. H. Li³⁹, Cheng Li^{71,58}, D. M. Li⁸⁰, F. Li^{1,58}, G. Li¹, H. Li^{71,58}, H. B. Li^{1,63}, H. J. Li¹⁹, H. N. Li^{56,i}, Hui Li⁴³, J. R. Li⁶¹, J. S. Li⁵⁹, Ke Li¹, L. J. Li^{1,63}, L. K. Li¹, Lei Li⁴⁸, M. H. Li⁴³, P. R. Li^{38,k}, Q. M. Li^{1,63}, Q. X. Li⁵⁰, R. Li^{17,31}, S. X. Li¹², T. Li⁵⁰, W. D. Li^{1,63}, W. G. Li¹, X. Li^{1,63}, X. H. Li^{71,58}, X. L. Li⁵⁰, Xiaoyu Li^{1,63}, Y. G. Li^{46,g}, Z. J. Li⁵⁹, Z. X. Li¹⁵, C. Liang⁴², H. Liang^{71,58}, H. Liang^{1,63}, Y. F. Liang⁵⁴, Y. T. Liang^{31,63}, G. R. Liao¹⁴, L. Z. Liao⁵⁰, Y. P. Liao^{1,63}, J. Libby²⁶, A. Limphirat⁶⁰, D. X. Lin^{31,63}, T. Lin¹, B. J. Liu¹, B. X. Liu⁷⁶, C. Liu³⁴, C. X. Liu¹, F. H. Liu⁵³, Fang Liu¹, Feng Liu⁶, G. M. Liu^{56,i}, H. Liu^{38,j,k}, H. B. Liu¹⁵, H. M. Liu^{1,63}, Huanhuan Liu¹, Huihui Liu²¹, J. B. Liu^{71,58}, J. Y. Liu^{1,63}, K. Liu^{38,j,k}, K. Y. Liu⁴⁰, Ke Liu²², L. Liu^{71,58}, L. C. Liu⁴³, Lu Liu⁴³, M. H. Liu^{12,f}, P. L. Liu¹, Q. Liu⁶³, S. B. Liu^{71,58}, T. Liu^{12,f}, W. K. Liu⁴³, W. M. Liu^{71,58}, X. Liu^{38,j,k}, X. Liu³⁹, Y. Liu^{38,j,k}, Y. Liu⁸⁰, Y. B. Liu⁴³, Z. A. Liu^{1,58,63}, Z. D. Liu⁹, Z. Q. Liu⁵⁰, X. C. Lou^{1,58,63}, F. X. Lu⁵⁹, H. J. Lu²³, J. G. Lu^{1,58}, X. L. Lu¹, Y. Lu⁷, Y. P. Lu^{1,58}, Z. H. Lu^{1,63}, C. L. Luo⁴¹, M. X. Luo⁷⁹, T. Luo^{12,f}, X. L. Luo^{1,58}, X. R. Lyu⁶³, Y. F. Lyu⁴³, F. C. Ma⁴⁰, H. Ma⁷⁸, H. L. Ma¹, J. L. Ma^{1,63}, L. L. Ma⁵⁰, M. M. Ma^{1,63}, Q. M. Ma¹, R. Q. Ma^{1,63}, X. T. Ma^{1,63}, X. Y. Ma^{1,58}, Y. Ma^{46,g}, Y. M. Ma³¹, F. E. Maas¹⁸, M. Maggiora^{74A,74C}, S. Malde⁶⁹, A. Mangoni^{28B}, Y. J. Mao^{46,g}, Z. P. Mao¹, S. Marcello^{74A,74C}, Z. X. Meng⁶⁶, J. G. Messchendorp^{13,64}, G. Mezzadri^{29A}, H. Miao^{1,63}, T. J. Min⁴², R. E. Mitchell²⁷, X. H. Mo^{1,58,63}, B. Moses²⁷, N. Yu. Muchnoi^{4,b}, J. Muskalla³⁵, Y. Nefedov³⁶, F. Nerling^{18,d}, I. B. Nikolaev^{4,b}, Z. Ning^{1,58}, S. Nisar^{11,l}, Q. L. Niu^{38,j,k}, W. D. Niu⁵⁵, Y. Niu⁵⁰, S. L. Olsen⁶³, Q. Ouyang^{1,58,63}, S. Pacetti^{28B,28C}, X. Pan⁵⁵, Y. Pan⁵⁷, A. Pathak³⁴, P. Patteri^{28A}, Y. P. Pei^{71,58}, M. Pelizaeus³, H. P. Peng^{71,58}, Y. Y. Peng^{38,j,k}, K. Peters^{13,d}, J. L. Ping⁴¹, R. G. Ping^{1,63}, S. Plura³⁵, V. Prasad³³, F. Z. Qi¹, H. Qi^{71,58}, H. R. Qi⁶¹, M. Qi⁴², T. Y. Qi^{12,f}, S. Qian^{1,58}, W. B. Qian⁶³, C. F. Qiao⁶³, X. K. Qiao⁸⁰, J. J. Qin⁷², L. Q. Qin¹⁴, X. S. Qin⁵⁰, Z. H. Qin^{1,58}, J. F. Qiu¹, S. Q. Qu⁶¹, Z. H. Qu⁷², C. F. Redmer³⁵, K. J. Ren³⁹, A. Rivetti^{74C}, M. Rolo^{74C}, G. Rong^{1,63}, Ch. Rosner¹⁸, S. N. Ruan⁴³, N. Salone⁴⁴, A. Sarantsev^{36,c}, Y. Schelhaas³⁵, K. Schoenning⁷⁵, M. Scodellaggio^{29A}, K. Y. Shan^{12,f}, W. Shan²⁴, X. Y. Shan^{71,58}, Z. J. Shang^{38,j,k}, J. F. Shangguan⁵⁵, L. G. Shao^{1,63}, M. Shao^{71,58}, C. P. Shen^{12,f}, H. F. Shen^{1,8}, W. H. Shen⁶³, X. Y. Shen^{1,63}, B. A. Shi⁶³, H. C. Shi^{71,58}, J. L. Shi¹², J. Y. Shi¹, Q. Q. Shi⁵⁵, R. S. Shi^{1,63}, S. Y. Shi⁷², X. Shi^{1,58}, J. J. Song¹⁹, T. Z. Song⁵⁹, W. M. Song^{34,1}, Y. J. Song¹², Y. X. Song^{46,g,m}, S. Sosio^{74A,74C}, S. Spataro^{74A,74C}, F. Stieler³⁵, Y. J. Su⁶³, G. B. Sun⁷⁶, G. X. Sun¹, H. Sun⁶³, H. K. Sun¹, J. F. Sun¹⁹, K. Sun⁶¹, L. Sun⁷⁶, S. S. Sun^{1,63}, T. Sun^{51,e}, W. Y. Sun³⁴, Y. Sun⁹, Y. J. Sun^{71,58}, Y. Z. Sun¹, Z. Q. Sun^{1,63}, Z. T. Sun⁵⁰, C. J. Tang⁵⁴, G. Y. Tang¹, J. Tang⁵⁹, Y. A. Tang⁷⁶, L. Y. Tao⁷², Q. T. Tao^{25,h}, M. Tat⁶⁹, J. X. Teng^{71,58}, V. Thoren⁷⁵, W. H. Tian⁵⁹, Y. Tian^{31,63}, Z. F. Tian⁷⁶, I. Uman^{62B}, Y. Wan⁵⁵, S. J. Wang⁵⁰, B. Wang¹, B. L. Wang⁶³, Bo Wang^{1,63}, D. Y. Wang^{46,g}, F. Wang⁷², H. J. Wang^{38,j,k}, J. P. Wang⁵⁰, K. Wang^{1,58}, L. L. Wang¹, M. Wang⁵⁰, Meng Wang⁶³, N. Y. Wang⁶³, S. Wang^{38,j,k}, S. Wang^{12,f}, T. Wang^{12,f}, T. J. Wang⁴³, W. Wang⁵⁹, W. Wang⁷², W. P. Wang^{71,58}, X. Wang^{46,g}, X. F. Wang^{38,j,k}, X. J. Wang³⁹, X. L. Wang^{12,f}, X. N. Wang¹, Y. Wang¹, Y. D. Wang⁴⁵, Y. F. Wang^{1,58,63}, Y. L. Wang¹⁹, Y. N. Wang⁴⁵, Y. Q. Wang¹, Yaqian Wang¹⁷, Yi Wang⁶¹, Z. Wang^{1,58}, Z. L. Wang⁷², Z. Y. Wang^{1,63}, Ziyi Wang⁶³, D. Wei⁷⁰, D. H. Wei¹⁴, F. Weidner⁶⁸, S. P. Wen¹, Y. R. Wen³⁹, U. Wiedner³, G. Wilkinson⁶⁹, M. Wolke⁷⁵, L. Wollenberg³, C. Wu³⁹, J. F. Wu^{1,8}, L. H. Wu¹, L. J. Wu⁶³, X. Wu^{12,f}, X. H. Wu³⁴, Y. Wu⁷¹, Y. H. Wu⁵⁵, Y. J. Wu³¹, Z. Wu^{1,58}, L. Xia^{71,58}, X. M. Xian³⁹, B. H. Xiang^{1,63}, T. Xiang^{46,g}, D. Xiao^{38,j,k}, G. Y. Xiao⁴², S. Y. Xiao¹, Y. L. Xiao^{12,f},

Z. J. Xiao⁴¹, C. Xie⁴², X. H. Xie^{46,g}, Y. Xie⁵⁰, Y. G. Xie^{1,58}, Y. H. Xie⁶, Z. P. Xie^{71,58}, T. Y. Xing^{1,63}, C. F. Xu^{1,63}, C. J. Xu⁵⁹, G. F. Xu¹, H. Y. Xu⁶⁶, Q. J. Xu¹⁶, Q. N. Xu³⁰, W. Xu¹, W. L. Xu⁶⁶, X. P. Xu⁵⁵, Y. C. Xu⁷⁷, Z. P. Xu⁴², Z. S. Xu⁶³, F. Yan^{12,f}, L. Yan^{12,f}, W. B. Yan^{71,58}, W. C. Yan⁸⁰, X. Q. Yan¹, H. J. Yang^{51,e}, H. L. Yang³⁴, H. X. Yang¹, Tao Yang¹, Y. Yang^{12,f}, Y. F. Yang⁴³, Y. X. Yang^{1,63}, Yifan Yang^{1,63}, Z. W. Yang^{38,j,k}, Z. P. Yao⁵⁰, M. Ye^{1,58}, M. H. Ye⁸, J. H. Yin¹, Z. Y. You⁵⁹, B. X. Yu^{1,58,63}, C. X. Yu⁴³, G. Yu^{1,63}, J. S. Yu^{25,h}, T. Yu⁷², X. D. Yu^{46,g}, Y. C. Yu⁸⁰, C. Z. Yuan^{1,63}, J. Yuan³⁴, L. Yuan², S. C. Yuan¹, Y. Yuan^{1,63}, Z. Y. Yuan⁵⁹, C. X. Yue³⁹, A. A. Zafar⁷³, F. R. Zeng⁵⁰, S. H. Zeng⁷², X. Zeng^{12,f}, Y. Zeng^{25,h}, Y. J. Zeng⁵⁹, Y. J. Zeng^{1,63}, X. Y. Zhai³⁴, Y. C. Zhai⁵⁰, Y. H. Zhan⁵⁹, A. Q. Zhang^{1,63}, B. L. Zhang^{1,63}, B. X. Zhang¹, D. H. Zhang⁴³, G. Y. Zhang¹⁹, H. Zhang⁷¹, H. C. Zhang^{1,58,63}, H. H. Zhang⁵⁹, H. H. Zhang³⁴, H. Q. Zhang^{1,58,63}, H. Y. Zhang^{1,58}, J. Zhang⁸⁰, J. J. Zhang⁵², J. L. Zhang²⁰, J. Q. Zhang⁴¹, J. W. Zhang^{1,58,63}, J. X. Zhang^{38,j,k}, J. Y. Zhang¹, J. Z. Zhang^{1,63}, Jianyu Zhang⁶³, L. M. Zhang⁶¹, Lei Zhang⁴², P. Zhang^{1,63}, Q. Y. Zhang^{39,80}, R. Y. Zhang^{38,j,k}, Shuihan Zhang^{1,63}, Shulei Zhang^{25,h}, X. D. Zhang⁴⁵, X. M. Zhang¹, X. Y. Zhang⁵⁰, Y. Zhang⁷², Y. T. Zhang⁸⁰, Y. H. Zhang^{1,58}, Y. M. Zhang³⁹, Yan Zhang^{71,58}, Yao Zhang¹, Z. D. Zhang¹, Z. H. Zhang¹, Z. L. Zhang³⁴, Z. Y. Zhang⁷⁶, Z. Y. Zhang⁴³, G. Zhao¹, J. Y. Zhao^{1,63}, J. Z. Zhao^{1,58}, Lei Zhao^{71,58}, Ling Zhao¹, M. G. Zhao⁴³, R. P. Zhao⁶³, S. J. Zhao⁸⁰, Y. B. Zhao^{1,58}, Y. X. Zhao^{31,63}, Z. G. Zhao^{71,58}, A. Zhemchugov^{36,a}, B. Zheng⁷², J. P. Zheng^{1,58}, W. J. Zheng^{1,63}, Y. H. Zheng⁶³, B. Zhong⁴¹, X. Zhong⁵⁹, H. Zhou⁵⁰, J. Y. Zhou³⁴, L. P. Zhou^{1,63}, X. Zhou⁷⁶, X. K. Zhou⁶, X. R. Zhou^{71,58}, X. Y. Zhou³⁹, Y. Z. Zhou^{12,f}, J. Zhu⁴³, K. Zhu¹, K. J. Zhu^{1,58,63}, L. Zhu³⁴, L. X. Zhu⁶³, S. H. Zhu⁷⁰, S. Q. Zhu⁴², T. J. Zhu^{12,f}, W. J. Zhu^{12,f}, Y. C. Zhu^{71,58}, Z. A. Zhu^{1,63}, J. H. Zou¹, J. Zu^{71,58}

(BESIII Collaboration)

¹ *Institute of High Energy Physics, Beijing 100049, People's Republic of China*

² *Beihang University, Beijing 100191, People's Republic of China*

³ *Bochum Ruhr-University, D-44780 Bochum, Germany*

⁴ *Budker Institute of Nuclear Physics SB RAS (BINP), Novosibirsk 630090, Russia*

⁵ *Carnegie Mellon University, Pittsburgh, Pennsylvania 15213, USA*

⁶ *Central China Normal University, Wuhan 430079, People's Republic of China*

⁷ *Central South University, Changsha 410083, People's Republic of China*

⁸ *China Center of Advanced Science and Technology, Beijing 100190, People's Republic of China*

⁹ *China University of Geosciences, Wuhan 430074, People's Republic of China*

¹⁰ *Chung-Ang University, Seoul, 06974, Republic of Korea*

¹¹ *COMSATS University Islamabad, Lahore Campus, Defence Road, Off Raiwind Road, 54000 Lahore, Pakistan*

¹² *Fudan University, Shanghai 200433, People's Republic of China*

¹³ *GSI Helmholtzcentre for Heavy Ion Research GmbH, D-64291 Darmstadt, Germany*

¹⁴ *Guangxi Normal University, Guilin 541004, People's Republic of China*

¹⁵ *Guangxi University, Nanning 530004, People's Republic of China*

¹⁶ *Hangzhou Normal University, Hangzhou 310036, People's Republic of China*

¹⁷ *Hebei University, Baoding 071002, People's Republic of China*

¹⁸ *Helmholtz Institute Mainz, Staudinger Weg 18, D-55099 Mainz, Germany*

¹⁹ *Henan Normal University, Xinxiang 453007, People's Republic of China*

²⁰ *Henan University, Kaifeng 475004, People's Republic of China*

²¹ *Henan University of Science and Technology, Luoyang 471003, People's Republic of China*

²² *Henan University of Technology, Zhengzhou 450001, People's Republic of China*

²³ *Huangshan College, Huangshan 245000, People's Republic of China*

²⁴ *Hunan Normal University, Changsha 410081, People's Republic of China*

²⁵ *Hunan University, Changsha 410082, People's Republic of China*

²⁶ *Indian Institute of Technology Madras, Chennai 600036, India*

²⁷ *Indiana University, Bloomington, Indiana 47405, USA*

²⁸ *INFN Laboratori Nazionali di Frascati, (A)INFN Laboratori Nazionali di Frascati, I-00044, Frascati, Italy; (B)INFN Sezione di Perugia, I-06100, Perugia, Italy; (C)University of Perugia, I-06100, Perugia, Italy*

²⁹ *INFN Sezione di Ferrara, (A)INFN Sezione di Ferrara, I-44122, Ferrara, Italy; (B)University of Ferrara, I-44122, Ferrara, Italy*

³⁰ *Inner Mongolia University, Hohhot 010021, People's Republic of China*

³¹ *Institute of Modern Physics, Lanzhou 730000, People's Republic of China*

³² *Institute of Physics and Technology, Peace Avenue 54B, Ulaanbaatar 13330, Mongolia*

³³ *Instituto de Alta Investigación, Universidad de Tarapacá, Casilla 7D, Arica 1000000, Chile*

³⁴ *Jilin University, Changchun 130012, People's Republic of China*

³⁵ *Johannes Gutenberg University of Mainz, Johann-Joachim-Becher-Weg 45, D-55099 Mainz, Germany*

³⁶ *Joint Institute for Nuclear Research, 141980 Dubna, Moscow region, Russia*

³⁷ *Justus-Liebig-Universitaet Giessen, II. Physikalisches Institut, Heinrich-Buff-Ring 16, D-35392 Giessen, Germany*

³⁸ *Lanzhou University, Lanzhou 730000, People's Republic of China*

³⁹ *Liaoning Normal University, Dalian 116029, People's Republic of China*

⁴⁰ *Liaoning University, Shenyang 110036, People's Republic of China*

⁴¹ *Nanjing Normal University, Nanjing 210023, People's Republic of China*

⁴² *Nanjing University, Nanjing 210093, People's Republic of China*

⁴³ Nankai University, Tianjin 300071, People's Republic of China
⁴⁴ National Centre for Nuclear Research, Warsaw 02-093, Poland
⁴⁵ North China Electric Power University, Beijing 102206, People's Republic of China
⁴⁶ Peking University, Beijing 100871, People's Republic of China
⁴⁷ Qufu Normal University, Qufu 273165, People's Republic of China
⁴⁸ Renmin University of China, Beijing 100872, People's Republic of China
⁴⁹ Shandong Normal University, Jinan 250014, People's Republic of China
⁵⁰ Shandong University, Jinan 250100, People's Republic of China
⁵¹ Shanghai Jiao Tong University, Shanghai 200240, People's Republic of China
⁵² Shanxi Normal University, Linfen 041004, People's Republic of China
⁵³ Shanxi University, Taiyuan 030006, People's Republic of China
⁵⁴ Sichuan University, Chengdu 610064, People's Republic of China
⁵⁵ Soochow University, Suzhou 215006, People's Republic of China
⁵⁶ South China Normal University, Guangzhou 510006, People's Republic of China
⁵⁷ Southeast University, Nanjing 211100, People's Republic of China
⁵⁸ State Key Laboratory of Particle Detection and Electronics, Beijing 100049, Hefei 230026, People's Republic of China
⁵⁹ Sun Yat-Sen University, Guangzhou 510275, People's Republic of China
⁶⁰ Suranaree University of Technology, University Avenue 111, Nakhon Ratchasima 30000, Thailand
⁶¹ Tsinghua University, Beijing 100084, People's Republic of China
⁶² Turkish Accelerator Center Particle Factory Group, (A)Istinye University, 34010, Istanbul, Turkey; (B)Near East University, Nicosia, North Cyprus, 99138, Mersin 10, Turkey
⁶³ University of Chinese Academy of Sciences, Beijing 100049, People's Republic of China
⁶⁴ University of Groningen, NL-9747 AA Groningen, The Netherlands
⁶⁵ University of Hawaii, Honolulu, Hawaii 96822, USA
⁶⁶ University of Jinan, Jinan 250022, People's Republic of China
⁶⁷ University of Manchester, Oxford Road, Manchester, M13 9PL, United Kingdom
⁶⁸ University of Muenster, Wilhelm-Klemm-Strasse 9, 48149 Muenster, Germany
⁶⁹ University of Oxford, Keble Road, Oxford OX13RH, United Kingdom
⁷⁰ University of Science and Technology Liaoning, Anshan 114051, People's Republic of China
⁷¹ University of Science and Technology of China, Hefei 230026, People's Republic of China
⁷² University of South China, Hengyang 421001, People's Republic of China
⁷³ University of the Punjab, Lahore-54590, Pakistan
⁷⁴ University of Turin and INFN, (A)University of Turin, I-10125, Turin, Italy; (B)University of Eastern Piedmont, I-15121, Alessandria, Italy; (C)INFN, I-10125, Turin, Italy
⁷⁵ Uppsala University, Box 516, SE-75120 Uppsala, Sweden
⁷⁶ Wuhan University, Wuhan 430072, People's Republic of China
⁷⁷ Yantai University, Yantai 264005, People's Republic of China
⁷⁸ Yunnan University, Kunming 650500, People's Republic of China
⁷⁹ Zhejiang University, Hangzhou 310027, People's Republic of China
⁸⁰ Zhengzhou University, Zhengzhou 450001, People's Republic of China

^a Also at the Moscow Institute of Physics and Technology, Moscow 141700, Russia
^b Also at the Novosibirsk State University, Novosibirsk, 630090, Russia
^c Also at the NRC "Kurchatov Institute", PNPI, 188300, Gatchina, Russia
^d Also at Goethe University Frankfurt, 60323 Frankfurt am Main, Germany
^e Also at Key Laboratory for Particle Physics, Astrophysics and Cosmology, Ministry of Education; Shanghai Key Laboratory for Particle Physics and Cosmology; Institute of Nuclear and Particle Physics, Shanghai 200240, People's Republic of China
^f Also at Key Laboratory of Nuclear Physics and Ion-beam Application (MOE) and Institute of Modern Physics, Fudan University, Shanghai 200443, People's Republic of China
^g Also at State Key Laboratory of Nuclear Physics and Technology, Peking University, Beijing 100871, People's Republic of China
^h Also at School of Physics and Electronics, Hunan University, Changsha 410082, China
ⁱ Also at Guangdong Provincial Key Laboratory of Nuclear Science, Institute of Quantum Matter, South China Normal University, Guangzhou 510006, China
^j Also at MOE Frontiers Science Center for Rare Isotopes, Lanzhou University, Lanzhou 730000, People's Republic of China
^k Also at Lanzhou Center for Theoretical Physics, Lanzhou University, Lanzhou 730000, People's Republic of China
^l Also at the Department of Mathematical Sciences, IBA, Karachi 75270, Pakistan
^m Also at Ecole Polytechnique Federale de Lausanne (EPFL), CH-1015 Lausanne, Switzerland

(Dated: May 7, 2025)

Using e^+e^- collision data corresponding to a total integrated luminosity of 22.7 fb^{-1} , collected at center-of-mass energies between 3.7 and 4.7 GeV with the BESIII detector, we present a measurement of energy-dependent cross sections and effective form factors for the process of $e^+e^- \rightarrow \Omega^-\bar{\Omega}^+$.

By conducting a fit to the cross sections of $e^+e^- \rightarrow \Omega^-\bar{\Omega}^+$ considering the continuum and resonant contributions, a clear resonant structure in the spectrum around 4.2 GeV is observed for the first time with a statistical significance exceeding 10σ , and it can be well described with the line shape of the $Y(4230)$ and $Y(4320)$ observed in $e^+e^- \rightarrow \pi^+\pi^-J/\psi$. Evidence for the decay $\psi(3770) \rightarrow \Omega^-\bar{\Omega}^+$ is observed with a statistical significance of 4.4σ by analyzing the measured cross sections together with earlier BESIII results, and the branching fraction is firstly measured to be $(4.0 \pm 1.0 \pm 0.6) \times 10^{-5}$, where the first uncertainty is statistical and the second is systematic.

Over the past two decades, several charmonium-like vector states, such as $Y(4220)$, $Y(4260)$, $Y(4360)$, and $Y(4660)$, have been observed by the BaBar [1–4], Belle [5–8], CLEO [9, 10], and BESIII [11–15] experiments. Numerous theoretical models have been proposed to decipher the nature of them. The interpretations include hybrid charmonia [16], tetraquarks [17], and hadronic molecules [18]. Yet, none of these models fully account for all experimental observations. These states typically couple to both open-charm and hidden-charm final states. Investigating their charmless decays, such as light hadronic and baryonic decays, could be essential for understanding their true nature. Recent efforts by BESIII have included searches for charmonium-like states within the context of light hadronic decay studies of $Z_c(3900)^\pm \rightarrow \omega\pi^\pm$ [19] and baryonic decay studies of $Y \rightarrow \Xi^-\bar{\Xi}^+$ and $\Lambda\bar{\Lambda}$ [20, 21]. However, these investigations have not yet yielded clear signals. Studies of the processes $e^+e^- \rightarrow D_s^{*+}D_s^{*-}$ [22] and $e^+e^- \rightarrow D_s^+D_s^-$ [23] at BESIII reveal that the observed charmonium-like Y -states couple strongly to final states containing strange quarks. To further interrogate the nature of these states and their potential exotic configurations (e.g., gluonic hybrids or tetraquarks), investigating channels with enhanced strangeness content is critical. The reaction $e^+e^- \rightarrow \Omega^-\bar{\Omega}^+$, where both the Ω^- and $\bar{\Omega}^+$ baryons each contain three strange quarks, offers a unique probe into the baryonic decay mechanisms of these Y -states.

The $\psi(3770)$ meson is believed to be a conventional $c\bar{c}$ state located above the open-charm threshold and is expected to dominantly decay into a $D\bar{D}$ meson pair. Experimental measurements from BES [24–27] reveal a significant non- $D\bar{D}$ branching fraction of $(14.7 \pm 3.2)\%$ [28], which exceeds theoretical predictions from conventional charmonium models (e.g., NRQCD calculations: 4% [29], NRQCD+FSI: 5.5–6.4% [30]). This discrepancy suggests either unaccounted dynamics in $c\bar{c}$ state decays or the presence of exotic components like four-quark admixtures [31], which could enhance non- $D\bar{D}$ decays. Searching for $e^+e^- \rightarrow \Omega^-\bar{\Omega}^+$ around 3.773 GeV could probe the hypothesized four-quark structure [32] or test the existence of additional structures near 3.773 GeV [33, 34], while also constraining models of strong interaction mechanisms in charmonium decays.

Furthermore, the measured Born cross sections (BCSs) can be applied for extracting the hyperon effective form factors (EFFs) [20, 21, 35], which are characterized

by four independent electromagnetic form factors, G_{E0} , G_{M1} , G_{E2} , and G_{M3} [36, 37]. Recent data from BESIII and CLEO-c provide important insights into time-like form factors at $\sqrt{s} \approx 3.7$ GeV [35, 38, 39]. A recent calculation of the EFF for the Ω^- hyperon was performed using the covariant spectator quark model [40] in higher energy range, more data specifically at high \sqrt{s} are therefore highly desirable to provide better constraints on the shape of the form factors.

In this Letter, we present a measurement of the BCS and the EFF for the $e^+e^- \rightarrow \Omega^-\bar{\Omega}^+$ process using 22.7 fb^{-1} of e^+e^- collision data collected at 34 center-of-mass (c.m.) energies from 3.7 to 4.7 GeV [41] with the BESIII detector. Combined with a previous measurement [35], the data above 3.7 GeV enables us to explore the baryonic decays of $\psi(3770)$ and vector charmonium-like state around 4.2 GeV by investigating the line shape of the $e^+e^- \rightarrow \Omega^-\bar{\Omega}^+$ process.

Details about the design and performance of the BESIII detector are given in Refs. [41, 42]. The Monte Carlo (MC) samples of 100,000 events for the $e^+e^- \rightarrow \Omega^-\bar{\Omega}^+$, $\Omega^- \rightarrow \Lambda K^-$, $\Lambda \rightarrow p\pi^-$, $\bar{\Omega}^+ \rightarrow$ anything are generated by KKMC generator under BESIII offline software from work Ref. [45]. The joint angular distribution of the decay sequence is used for each of the 34 c.m. energy points. Unless explicitly stated, charge-conjugate modes are always implied throughout this Letter. The decay modes of the Ω^- hyperon are generated using EVTGEN [46], with branching fractions set to the world average values [47]. Additionally, extensive generic decay MC samples are utilized to estimate background contributions.

A single baryon tag method is employed to select $e^+e^- \rightarrow \Omega^-\bar{\Omega}^+$ candidate events, where only one baryon from the $\Omega^-\bar{\Omega}^+$ pair is reconstructed in each event. The baryon or antibaryon on the recoil side is inferred from the recoil mass of the reconstructed particles. The following event selection criteria are detailed for the decay $\Omega^- \rightarrow K^-\Lambda$ ($\Lambda \rightarrow p\pi^-$) as an example. Identical selection criteria are applied to the $\bar{\Omega}^+$ case. Charged proton, kaon, and pion candidates are reconstructed with the criteria as shown in Ref. [48]. Events with at least one proton, kaon, and pion candidate are kept for further analysis.

Each Λ (Ω^-) candidate is reconstructed from a pair of $p\pi^-$ ($K^-\Lambda$) candidates that are constrained to originate from a common vertex by requiring the χ^2 of the vertex fit to be less than 100. A loose requirement is placed

on Λ invariant mass, $1.09 < M(p\pi^-) < 1.14 \text{ GeV}/c^2$, to suppress background events. The distance between the e^+e^- interaction point and the decay vertices of the Λ (Ω^-) candidates, is required to exceed twice the fitted uncertainties. In cases where more than one Ω^- or $\bar{\Omega}^+$ candidate meets all these criteria within the same event, the candidate with the lowest vertex fit χ^2 value is retained. The $M(p\pi^-)$ is further constrained to the Λ signal region of $[1.111, 1.121] \text{ GeV}/c^2$ corresponds to three times the $p\pi^-$ mass resolution relative to the nominal Λ mass [47]. Fig. 1 illustrates the distribution of $RM^{\text{cor}}(K^-\Lambda)$ versus $M^{\text{cor}}(K^-\Lambda)$ for the events having passed all the aforementioned criteria, summed over all data samples, where $RM^{\text{cor}}(K^-\Lambda) = RM(K^-\Lambda) + M(K^-\Lambda) - m(\Omega^-)$ and $M^{\text{cor}}(K^-\Lambda) = M(K^-\Lambda) - M(p\pi^-) + m(\Lambda)$. Here, $M(K^-\Lambda)$ represents the invariant mass of the $K^-\Lambda$ combination, and $m(\Lambda)$ ($m(\Omega^-)$) is the known mass of the Λ (Ω^-) as provided by the PDG [47]. A pronounced enhancement around the nominal Ω^- mass is observed.

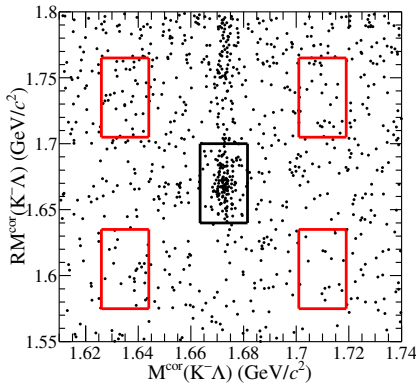


FIG. 1. Distribution of $RM^{\text{cor}}(K^-\Lambda)$ versus $M^{\text{cor}}(K^-\Lambda)$ of the accepted candidates from all 34 data sets, where the black box shows the signal region, and the red boxes denote the selected sideband regions.

After applying the criteria introduced previously, the remaining background events originate mainly from non- Ω processes, such as $e^+e^- \rightarrow \Lambda\bar{\Lambda}\phi$ with $\phi \rightarrow K^-K^+$. The background contribution within the signal region is estimated using four sideband regions, each having the same area as the signal region. These regions are depicted in Fig. 1. The signal region is defined as $[1.6635, 1.6815] \text{ GeV}/c^2$ for $M^{\text{cor}}(K^-\Lambda)$, corresponding to three times the mass resolution on the tag side, and $[1.64, 1.70] \text{ GeV}/c^2$ for $RM^{\text{cor}}(K^-\Lambda)$ on the recoil side, as determined from MC simulations. The sideband regions are specified as $[1.626, 1.644]$ and $[1.701, 1.719] \text{ GeV}/c^2$ for $M^{\text{cor}}(K^-\Lambda)$ and $[1.575, 1.635] \text{ GeV}/c^2$ and $[1.705, 1.765] \text{ GeV}/c^2$ for $RM^{\text{cor}}(K^-\Lambda)$. The net signal yield (N^{sig}) at each c.m. energy is computed by subtracting the normalized total number of events in the sideband regions (N^{bkg}) from the number of events in the signal region

(N^{obs}), using the formula $N^{\text{sig}} = N^{\text{obs}} - \frac{1}{4} N^{\text{bkg}}$. Any negative values of N^{sig} are set to zero to avoid an unphysical count of signal events. The statistical uncertainties for N^{sig} are determined using the TRolke package [49]. The upper limit N^{UL} at a 90% confidence level is calculated for any data set with statistical significance below 3σ , after accounting for systematic uncertainties. Comprehensive numerical results are provided in Table I of the Supplemental Material [50].

The BCS of the $e^+e^- \rightarrow \Omega^-\bar{\Omega}^+$ process at each c.m. energy is calculated with

$$\sigma^{\text{B}} = \frac{N^{\text{sig}}}{\mathcal{L}(1 + \delta) \frac{1}{|1 - \Pi|^2} \mathcal{B}(\Omega^- \rightarrow K^-\Lambda) \mathcal{B}(\Lambda \rightarrow p\pi^-) \epsilon},$$

where N^{sig} is the net signal yield, \mathcal{L} is the integrated luminosity, ϵ is the detection efficiency, $(1 + \delta)$ is the ISR correction factor, and $(1/|1 - \Pi|^2)$ is the correction factor for vacuum polarization [51]. $\mathcal{B}(\Omega^- \rightarrow K^-\Lambda)$ and $\mathcal{B}(\Lambda \rightarrow p\pi^-)$ denote the branching fractions of $\Omega^- \rightarrow K^-\Lambda$ and $\Lambda \rightarrow p\pi^-$, respectively [47]. The ISR correction factors and detection efficiencies are derived from MC simulations and are corrected by an iterative weighting method [52].

The energy-dependent EFF could be extracted from the total BCS by [35]

$$|G_{\text{eff}}(s)| = \sqrt{\frac{3s\sigma^{\text{B}}}{4\pi\alpha^2\mathcal{C}\beta(1 + \frac{2m_{\Omega}^2}{s})}},$$

where s is the squared c.m. energy, α is the fine structure constant, the variable $\beta = \sqrt{1 - \frac{4m_{\Omega}^2}{s}}$ is the velocity of Ω^- , and the Coulomb factor \mathcal{C} parameterizes the electromagnetic interaction between the outgoing baryon and the anti-baryon [53].

The measured cross sections and EFFs at the 34 c.m. energies are presented in Fig. 3, detailed values are listed in Table II of the Supplemental Material [50]. The upper limits are determined using the profile likelihood method, incorporating systematic uncertainties as outlined in Ref. [49]. Fig. 2 compares the EFFs determined in this study with those from CLEO-c measurements [38] and theoretical predictions based on the covariant spectator quark model [40]. The calculated EFFs are consistent with the theoretical predictions, with a discrepancy no greater than 1.0σ .

The systematic uncertainties in the BCS measurement primarily arise from several sources: the luminosity measurement, the branching fractions of the decays $\Omega^- \rightarrow K^-\Lambda$ and $\Lambda \rightarrow p\pi^-$, the reconstruction efficiency of the Ω^- , the MC generator, the mass windows for Λ and Ω^- selections, the choice of sideband regions and the estimation of $(1 + \delta)\epsilon$. Each of these sources of uncertainty is elaborated upon below. The integrated luminosity is

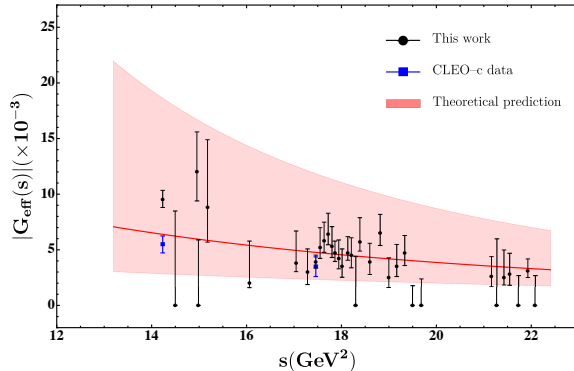


FIG. 2. Comparison of the measured EFFs and the theoretical prediction. The black points with error bars are the results of this work. The blue points with error bars are the CLEO-c measurements [38], where G_{E0} is assumed to be zero. The red band indicates the theoretical prediction, in which the red line denotes the predicted central value [40], and the CLEO-c results are used to fix the free parameters of the model.

determined using Bhabha events, with an uncertainty of 1.0% [54]. The uncertainties in the branching fractions of $\Omega^- \rightarrow K^- \Lambda$ and $\Lambda \rightarrow p\pi^-$ are taken from the PDG [47]. The systematic uncertainty related to the Ω reconstruction efficiency, which includes the tracking and PID efficiencies of charged tracks as well as the efficiency for Λ reconstruction, is estimated using a control sample from the decay $\psi' \rightarrow \Omega^- \bar{\Omega}^+$, following the method detailed in Ref. [20]. Additionally, we assess the systematic uncertainties due to the decay parameters (α_Ω and α_Λ) in the angular distribution function, and the helicity parameters derived from $\psi' \rightarrow \Omega^- \bar{\Omega}^+$ analysis [45], as part of the MC generator uncertainties. The uncertainties associated with the $M(p\pi^-)$ and $M^{\text{cor}}(K^- \Lambda)$ mass windows are assessed by employing an alternative selection condition, extending the range by $+1\sigma$. The uncertainty of the $RM^{\text{cor}}(K^- \Lambda)$ mass window is determined by reducing it by 0.01 GeV/c^2 . To estimate the uncertainty from the sideband positions, we double the relative positions of the signal and sideband regions. After adjusting the box window, we compare the signal yield from data and efficiency from MC simulation. The relative difference between the signal yield ratio from the data and the efficiency ratio from MC is used as the systematic uncertainty [55, 56]. The line shape of the cross-section contributes uncertainties to both ISR and the signal efficiency. The largest relative difference in $(1 + \delta)\epsilon$ is found to be 0.004% during the final two iterations, which is negligible. To evaluate the systematic uncertainty related to the input cross-section line-shape, we change the method of parameterization of the energy-dependent cross section (as illustrated in Fig. 3 and explained below). The relative difference in $(1 + \delta)\epsilon$ at each energy point is designated as the systematic uncertainty. Assuming all sources of uncertainty are independent, the

total relative systematic uncertainties at different energy points range from 5.6% to 5.7%, obtained by adding these uncertainties in quadrature.

The dressed cross sections, $\sigma^{\text{Dress}} = \sigma^B / |1 - \Pi|^2$, measured at various energy points are displayed in Fig. 3. Three potential enhancements are observed around 3.77, 4.20, and 4.30 GeV. To estimate the resonant contribution to the $e^+e^- \rightarrow \Omega^- \bar{\Omega}^+$ cross section, we fit the c.m. energy-dependent dressed cross section using results from this measurement and those at $\sqrt{s} < 3.77$ GeV in Ref. [35]. The fit employs a model that combines both continuum and resonant components and is performed using a maximum likelihood method. Details of the likelihood approach are provided in the Supplemental Material [50].

Assuming that the $\Omega^- \bar{\Omega}^+$ signals originate from two resonances near 3.7 and 4.2 GeV, as well as from a continuum process, we employ a model that combines two Breit-Wigner (BW) functions with a perturbative QCD (pQCD)-driven energy power function [35, 57, 58] to fit the measured cross sections. The model is expressed as follows:

$$\sigma^{\text{Dress}}(\sqrt{s}) = \left| \sqrt{\frac{c_0 \cdot \beta \cdot \mathcal{C}}{(\sqrt{s} - c_1)^{10}}} + e^{i\phi_1} B_1(\sqrt{s}) \sqrt{\frac{P(\sqrt{s})}{P(M_1)}} \right|^2 + \left| B_2(\sqrt{s}) \sqrt{\frac{P(\sqrt{s})}{P(M_2)}} \right|^2,$$

where c_0 and c_1 are fixed parameters based on the studies in Ref. [35]. The BW function B_i is defined as $B_i(\sqrt{s}) = \frac{\sqrt{12\pi(\Gamma_i^{ee}\mathcal{B}_i)\Gamma_{\text{tot},i}}}{s - M_i^2 + iM_i\Gamma_{\text{tot},i}}$, and $P(\sqrt{s})$ represents the two-body phase space factor. In the fitting process, the mass M_1 and total width $\Gamma_{\text{tot},1}$ are fixed to the parameters of $\psi(3770)$ according to the PDG [47], the products of the electronic partial width and the branching fraction to $\Omega^- \bar{\Omega}^+$ ($\Gamma_i^{ee}\mathcal{B}_i$), the mass M_2 and total width $\Gamma_{\text{tot},2}$, as well as the relative phase ϕ are treated as free parameters. Under this assumption, the parameters of $Y(4230)$ are determined to be $M = (4215.5 \pm 24.5)$ MeV/ c^2 and $\Gamma_{\text{tot}} = (215.5 \pm 55.0)$ MeV as shown in the upper plot of Fig. 3. The change in the likelihood value from the two resonances ($\psi(3770) + Y(4230)$) model compared to just one resonance ($\psi(3770)$) model is $|\Delta(-2 \ln L)| = 185.7$. Considering the change in the number of degrees of freedom ($\Delta\text{ndf} = 3$), the significance of the $Y(4230)$ is calculated to be approximately 13.2σ , indicating the presence of one or more structures around 4.2 GeV. By comparing fits with and without $\psi(3770)$ component, which gives $|\Delta(-2 \ln L)| = 22.7$ and $\Delta\text{ndf} = 2$, the statistical significance of $\psi(3770)$ is determined to be 4.4σ .

To improve the fit quality, an additional resonance around 4.3 GeV has been incorporated into the model. Consequently, the cross section is now parameterized as a

combination of three BW functions alongside an energy power function. The line shape of the cross section is described by

$$\sigma^{\text{Dress}}(\sqrt{s}) = \left| \sqrt{\frac{c_0 \cdot \beta \cdot \mathcal{C}}{(\sqrt{s} - c_1)^{10}}} + e^{i\phi_1} B_1(\sqrt{s}) \sqrt{\frac{P(\sqrt{s})}{P(M_1)}} \right|^2 + \left| B_2(\sqrt{s}) \sqrt{\frac{P(\sqrt{s})}{P(M_2)}} + e^{i\phi_2} B_3(\sqrt{s}) \sqrt{\frac{P(\sqrt{s})}{P(M_3)}} \right|^2.$$

The mass and width of $B_2(\sqrt{s})$ and $B_3(\sqrt{s})$ are fixed according to the parameters for $Y(4230)$ and $Y(4320)$ as provided in Ref. [59]. Specifically, M_2 is set to 4221.4 MeV/ c^2 with $\Gamma_{\text{tot},2} = 41.8$ MeV, and M_3 is set to 4298.0 MeV/ c^2 with $\Gamma_{\text{tot},3} = 127.0$ MeV. The products of the $\Gamma_i^{\text{ee}} \mathcal{B}_i$ and the relative phase ϕ are treated as free parameters. The interferences between $\psi(3770)$ and the other two BWs are neglected due to the significant separation and only the interference with continuum process is considered.

Under this assumption, there are two solutions for $\Gamma_{\text{ee}} \mathcal{B}(Y(4230))$ and $\Gamma_{\text{ee}} \mathcal{B}(Y(4320))$ measurements. One corresponds to constructive interference (solution I) and the other corresponds to destructive interference (solution II), as depicted in the lower plot of Fig. 3, with $|- \ln L| = 81.7$ and $\text{ndf} = 5$. For the interference between the $\psi(3770)$ resonance and the continuum process, only one solution is identified. The statistical significances of $\psi(3770)$, $Y(4230)$, and $Y(4320)$ are determined to be 4.5σ , 4.4σ , and 6.5σ , respectively, based on the differences in likelihood values and ndf , with and without the inclusion of the respective resonance. The hypothesis of including two resonances, $Y(4230)$ and $Y(4320)$, around 4.2 GeV, as opposed to no resonance in this region, shows a significance of 13.2σ using the same evaluation method. The products of the $\Gamma_{\text{ee}} \mathcal{B}$ for the states $\psi(3770)$, $Y(4230)$, and $Y(4320)$ are detailed in Table I. Assuming $\mathcal{B}(\psi(3770) \rightarrow e^+ e^-) = 9.6 \times 10^{-6}$, following the world average from the PDG [47], the branching fraction for the decay $\mathcal{B}(\psi(3770) \rightarrow \Omega^- \bar{\Omega}^+)$ is measured to be $(4.0 \pm 1.0) \times 10^{-5}$, with uncertainty being statistical only.

The systematic uncertainties associated with the measurements of $\Gamma_{\text{ee}} \mathcal{B}$ are discussed as follows. Deviations in the measured c.m. energy primarily affect mass measurements, and the systematic uncertainties related to $\Gamma_{\text{ee}} \mathcal{B}$ and the phase angle from this source can be neglected. The uncertainty in the beam spread is accounted for by smearing the c.m. energy with its uncertainty, modeled as $0.00067 \times \sqrt{s} - 0.00152$ GeV at each energy point. The uncertainties arising from the resonance parameters of $\psi(3770)$, $Y(4230)$, and $Y(4320)$ are assessed by varying these parameters within their uncertainties as listed by the PDG [47]. Interference effects between the continuum

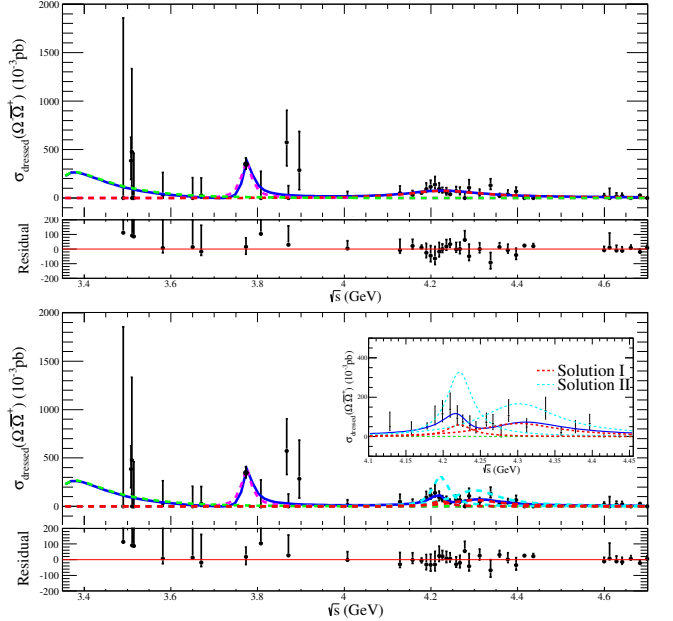


FIG. 3. Fits of dressed cross sections of $e^+e^- \rightarrow \Omega^-\bar{\Omega}^+$ and the residual distributions. The dots with error bars are data measured from this analysis together with earlier BESIII results [35]. The solid (blue) curves represent the fit results with the amplitudes of dashed pink lines ($\psi(3770)$) and dashed green lines (pQCD). Upper plot: assuming two resonances ($\psi(3770) + Y(4230)$ (dashed red line)). Lower plot: assuming three resonances ($\psi(3770) + Y(4230) + Y(4320)$) with combination of $Y(4230)$ and $Y(4320)$ for solution I (dashed red lines) and solution II (dashed light blue lines). The insert plot is the zoomed-in result around 4.2 GeV.

TABLE I. The parameters of the three resonances in the dressed cross section of $e^+e^- \rightarrow \Omega^-\bar{\Omega}^+$. Here the first uncertainty is statistical and the second is systematic.

Parameters	SolutionI	SolutionII
M_1 (MeV/ c^2)	3773.7 (fixed)	
Γ_1 (MeV)	27.2 (fixed)	
M_2 (MeV/ c^2)	4221.4 (fixed)	
Γ_2 (MeV)	41.8 (fixed)	
M_3 (MeV/ c^2)	4298.0 (fixed)	
Γ_3 (MeV)	127.0 (fixed)	
$\Gamma_{\text{ee}} \mathcal{B}(\psi(3770))$ (10 ⁻³ eV)	$10.5 \pm 2.5 \pm 1.4$	
$\Gamma_{\text{ee}} \mathcal{B}(Y(4230))$ (10 ⁻³ eV)	$3.0 \pm 1.2 \pm 0.8$	$16.6 \pm 2.4 \pm 9.2$
$\Gamma_{\text{ee}} \mathcal{B}(Y(4320))$ (10 ⁻³ eV)	$10.6 \pm 2.8 \pm 5.4$	$26.6 \pm 3.8 \pm 14.9$
ϕ_1 (rad)	$-0.3 \pm 0.7 \pm 0.1$	
ϕ_2 (rad)	$-0.3 \pm 0.3 \pm 0.8$	$-2.2 \pm 0.1 \pm 0.3$

and all three BW components are taken into account, and an alternative representation of the continuum contribution is used to estimate the systematic uncertainty. Each of these scenarios is applied individually to fit the cross-section line shape, with the largest resultant differences reported as the systematic uncertainties of the fit model. The uncertainties in the cross-section measurements are

estimated by including the correlated and uncorrelated systematic uncertainties of the measured cross sections in the fit [60]. The total systematic uncertainty is calculated by summing all sources of systematic uncertainties in quadrature, assuming they are uncorrelated as listed in Table III in the Supplemental Material [50].

In summary, using 22.7 fb^{-1} of e^+e^- collision data collected across 34 c.m. energies from 3.7 to 4.7 GeV with the BESIII detector, we determine the Born cross sections and effective form factors for the process $e^+e^- \rightarrow \Omega^-\bar{\Omega}^+$ using a single baryon tag method. The dressed cross sections are described by a coherent energy power function, alongside the $\psi(3770)$ and two coherent BW functions for the $Y(4230)$ and $Y(4320)$. The resonances around 4.2 and 4.3 GeV exhibit significances exceeding 10σ after accounting for systematic uncertainties. This is achieved by setting their parameters to the masses and widths of $Y(4230)$ and $Y(4320)$ according to Ref. [59]. The data suggest the necessity of including multiple Y structures, as evidenced by the more accurate fit achieved with two BW functions around 4.2 GeV compared to using just one BW function. Further data in this energy region could better clarify the couplings between Y states and the $\Omega^-\bar{\Omega}^+$ final states. Evidence of the decay $\psi(3770) \rightarrow \Omega^-\bar{\Omega}^+$ is observed with a significance of 4.4σ , factoring in all systematic uncertainties and combining the measured cross sections with previous BESIII results. The branching fraction is firstly determined to be $(4.0 \pm 1.0 \pm 0.6) \times 10^{-5}$, where the first uncertainty is statistical and the second is systematic. This value is larger by at least an order of magnitude than the prediction from Ref. [38], suggesting the non-negligible $\psi(3770)$ resonance contribution when interpreting the cross section of $e^+e^- \rightarrow \Omega^-\bar{\Omega}^+$. We also report on the product of $\Gamma_{ee}\mathcal{B}$ for $Y(4230)$ and $Y(4320)$. Our results provide strong evidence of resonant contributions in the decay process $e^+e^- \rightarrow \Omega^-\bar{\Omega}^+$, potentially marking the first observed baryonic decay mode of the charmonium-like state.

The BESIII Collaboration thanks the staff of BEPCII (<https://cstr.cn/31109.02.BEPC>) and the IHEP computing center for their strong support. This work is supported in part by National Key R&D Program of China under Contracts Nos. 2023YFA1606704, 2023YFA1606000; National Natural Science Foundation of China (NSFC) under Contracts Nos. 11635010, 11935015, 11935016, 11935018, 12025502, 12035009, 12035013, 12061131003, 12192260, 12192261, 12192262, 12192263, 12192264, 12192265, 12221005, 12225509, 12235017, 12361141819; the Chinese Academy of Sciences (CAS) Large-Scale Scientific Facility Program; CAS under Contract No. YSBR-101; 100 Talents Program of CAS; The Institute of Nuclear and Particle Physics (INPAC) and Shanghai Key Laboratory for Particle Physics and Cosmology; Agencia Nacional de In-

vestigación y Desarrollo de Chile (ANID), Chile under Contract No. ANID PIA/APOYO AFB230003; ERC under Contract No. 758462; German Research Foundation DFG under Contract No. FOR5327; Istituto Nazionale di Fisica Nucleare, Italy; Knut and Alice Wallenberg Foundation under Contracts Nos. 2021.0174, 2021.0299; Ministry of Development of Turkey under Contract No. DPT2006K-120470; National Research Foundation of Korea under Contract No. NRF-2022R1A2C1092335; National Science and Technology fund of Mongolia; Polish National Science Centre under Contract No. 2024/53/B/ST2/00975; STFC (United Kingdom); Swedish Research Council under Contract No. 2019.04595; U. S. Department of Energy under Contract No. DE-FG02-05ER41374.

- [1] J. P. Lees *et al.* (BaBar Collaboration), *Phys. Rev. Lett.* **95**, 142001 (2005).
- [2] J. P. Lees *et al.* (BaBar Collaboration), *Phys. Rev. Lett.* **98**, 212001 (2007).
- [3] J. P. Lees *et al.* (BaBar Collaboration), *Phys. Rev. D* **86**, 051102(R) (2012).
- [4] J. P. Lees *et al.* (BaBar Collaboration), *Phys. Rev. D* **89**, 111103(R) (2014).
- [5] X.L. Wang *et al.* (Belle Collaboration), *Phys. Rev. Lett.* **99**, 142002 (2007).
- [6] C.Z. Yuan *et al.* (Belle Collaboration), *Phys. Rev. Lett.* **99**, 182004 (2007).
- [7] Z.Q. Liu *et al.* (Belle Collaboration), *Phys. Rev. Lett.* **110**, 252002 (2013).
- [8] X.L. Wang *et al.* (Belle Collaboration), *Phys. Rev. D* **91**, 112007 (2015).
- [9] T.E. Coan *et al.* (CLEO Collaboration), *Phys. Rev. Lett.* **96**, 162003 (2006).
- [10] Q. He *et al.* (CLEO Collaboration), *Phys. Rev. D* **74**, 091104 (R) (2006).
- [11] C. Z. Yuan, *Chin. Phys. C* **38**, (4) 043001 (2014).
- [12] M. Ablikim *et al.* (BESIII Collaboration), *Phys. Rev. Lett.* **114**, 092003 (2015).
- [13] M. Ablikim *et al.* (BESIII Collaboration), *Phys. Rev. D* **91**, 112005 (2015).
- [14] M. Ablikim *et al.* (BESIII Collaboration), *Phys. Rev. Lett.* **118**, 092001 (2017).
- [15] M. Ablikim *et al.* (BESIII Collaboration), *Phys. Rev. D* **104**, 052012 (2021).
- [16] F. E. Close and P. R. Page, *Phys. Lett. B* **628**, 215–222 (2005).
- [17] L. Maiani, V. Riquer, F. Piccinini and A. D. Polosa, *Phys. Rev. D* **72**, 031502(R) (2005).
- [18] X. Liu, X. Q. Zeng and X. Q. Li, *Phys. Rev. D* **72**, 054023 (2005).
- [19] M. Ablikim *et al.* (BESIII Collaboration), *Phys. Rev. D* **92**, 032009(2015).
- [20] M. Ablikim *et al.* (BESIII Collaboration), *Phys. Rev. D* **104**, L091104 (2021).
- [21] M. Ablikim *et al.* (BESIII Collaboration), *Phys. Rev. Lett.* **124**, 032002 (2020).
- [22] M. Ablikim *et al.* (BESIII Collaboration), *Phys. Rev.*

Lett. **131**, 151903 (2023).

[23] M. Ablikim *et al.* (BESIII Collaboration), Phys. Rev. Lett. **133**, 261902 (2024).

[24] M. Ablikim *et al.* (BES Collaboration), Phys. Rev. Lett. **97**, 121801 (2006).

[25] M. Ablikim *et al.* (BES Collaboration), Phys. Lett. B **641**, 145-155 (2006).

[26] M. Ablikim *et al.* (BES Collaboration), Phys. Lett. B **659**, 74-79 (2008).

[27] M. Ablikim *et al.* (BES Collaboration), Phys. Rev. D **76**, 122002 (2007).

[28] G. Rong and D. Zhang and J. C. Chen, arXiv:1003.3523.

[29] Z. G. He, Y. Fan and K. T. Chao, Phys. Rev. Lett. **101**, 112001 (2008).

[30] X. Liu, B. Zhang and X. Q. Li, Phys. Lett. B **675**, 441-445 (2009).

[31] M. B. Voloshin, Phys. Rev. D **71**, 114003 (2005).

[32] M. B. Voloshin, Prog. Part. Nucl. Phys. **61**, 455-511 (2008).

[33] M. Ablikim *et al.* (BES Collaboration), Phys. Rev. Lett. **101**, 102004 (2008).

[34] S. Dubynskiy and M. B. Voloshin, Phys. Rev. D **78**, 116014 (2008).

[35] M. Ablikim *et al.* (BESIII Collaboration), Phys. Rev. D **10**, 052003 (2023).

[36] S. Nozawa and D. B. Leinweber, Phys. Rev. D **42**, 3567-3571 (1990).

[37] J. G. Korner and M. Kuroda, Phys. Rev. D **16**, 2165 (1977).

[38] S. Dobbs, Kamal K. Seth, A. Tomaradze, T. Xiao, and G. Bonvicini, Phys. Rev. D **96**, 092004 (2017).

[39] S. Dobbs, A. Tomaradze, T. Xiao, K. K. Seth and G. Bonvicini, Phys. Lett. B **739**, 90 (2014).

[40] G. RamalhoK, Phys. Rev. D **103**, 074018 (2021).

[41] M. Ablikim *et al.*, (BESIII Collaboration), Chin. Phys. C **44**, 040001 (2020).

[42] M. Ablikim *et al.* (BESIII Collaboration), Nucl. Instrum. Methods Phys. Res., Sect. A **614**, 345 (2010).

[43] S. Agostinelli *et al.* (GEANT4 Collaboration), Nucl. Instrum. Methods Phys. Res., Sect. A **506**, 250 (2003).

[44] S. Jadach, B. F. L. Ward and Z. Was, Phys. Rev. D **63**, 113009 (2001); Comput. Phys. Commun. **130**, 260 (2000).

[45] M. Ablikim *et al.* (BESIII Collaboration), Phys. Rev. Lett. **126**, 092002 (2021).

[46] D. J. Lange, Nucl. Instrum. Methods Phys. Res., Sect. A **462**, 152 (2001); R. G. Ping, Chin. Phys. C **32**, 599 (2008).

[47] S. Navas *et al.* (Particle Data Group), Phys. Rev. D **110**, 030001 (2024).

[48] M. Ablikim *et al.* (BESIII Collaboration), Phys. Rev. Lett. **134**, 131903 (2025).

[49] J. Lundberg, J. Conrad, W. Rolke and A. Lopez, Comput. Phys. Commun. **181**, 683 (2010).

[50] See Supplemental Material: for a summary of c.m. energies, integrated luminosities, number of signal events (their upper limits), event selection efficiencies, ISR correction factors, vacuum polarization factors, Born cross section and effective form factor at each energy point, definition of the likelihood used in the fit to the dressed cross section, and systematic uncertainty in the measurement of resonance parameters.

[51] S. Actis *et al.*, Eur. Phys. J. C **66**, 585 (2010).

[52] W. Sun, T. Liu, M. Jing, L. Wang, B. Zhong, and W. Song, Front. Phys. **16**, 64501 (2021).

[53] R. Baldini, S. Pacetti, A. Zallo and A. Zichichi, Eur. Phys. J. A **39**, 315 (2009).

[54] M. Ablikim *et al.* (BESIII Collaboration), Chin. Phys. C **39**(9), 093001 (2015).

[55] M. Ablikim *et al.* (BESIII Collaboration), Phys. Rev. D **87**, 032007 (2013).

[56] M. Ablikim *et al.* (BESIII Collaboration), Phys. Rev. D **100**, 051101 (2019).

[57] M. Ablikim *et al.* (BESIII Collaboration), Phys. Rev. D **97**, 032013 (2018).

[58] M. Ablikim *et al.* (BESIII Collaboration), Phys. Rev. D **103**, 012005 (2021).

[59] M. Ablikim *et al.* (BESIII Collaboration), Phys. Rev. D **106** (7), 072001 (2022).

[60] M. Ablikim *et al.* (BESIII Collaboration), Phys. Rev. Lett. **131**, 211902 (2023).